Research Article

Journal of PeptideScience

Received: 11 January 2011 Accepted: 18 January 2011 Published online in Wiley Online Library: 14 April 2011

(wileyonlinelibrary.com) DOI 10.1002/psc.1364

Synthesis, preferred conformation, protease stability, and membrane activity of heptaibin, a medium-length peptaibiotic

Marta De Zotti,[a]* Barbara Biondi,[a] Cristina Peggion,[a] Yoonkyung Park,[b,c] Kyung-Soo Hahm,[c,d] Fernando Formaggio[a] and Claudio Toniolo[a]

The medium-length peptaibiotics are characterized by a primary structure of 14–16 amino acid residues. Despite the interesting antibiotic and antifungal properties exhibited by these membrane-active peptides, their exact mechanism of action is still unknown. Here, we present our results on heptaibin, a 14-amino acid peptaibiotic found to exhibit antimicrobial activity against *Staphylococcus aureus*. We carried out the very challenging synthesis of heptaibin on solid phase and a detailed conformational analysis in solution. The peptaibiotic is folded in a mixed 3_{10}-/α-helix conformation which exhibits a remarkable amphiphilic character. We also find that it is highly stable toward degradation by proteolytic enzymes and nonhemolytic. Finally, fluorescence leakage experiments using small unilamellar vesicles of three different compositions revealed that heptaibin, although uncharged, is a selective compound for permeabilization of model membranes mimicking the overall negatively charged surface of Gram-positive bacteria. This latter finding is in agreement with the originally published antimicrobial activity data.

Supporting information may be found in the online version of this article

Keywords: α-aminoisobutyric acid; antibiotics; helical structure; membrane activity; peptides

Introduction

Antimicrobial peptides (AMPs) are well-known components of the innate immune system. In the family of AMPs, there is a class of naturally occurring peptides termed peptaibiotics [1] which are rich in noncoded α-amino acids (e.g. α-aminoisobutyric acid, Aib) and possess a C-terminal 1,2-aminoalcohol. Peptaibiotics are tipically divided in three subclasses, depending upon the length of their primary structure: (i) short-sequence (less than 11 residues), such as trichogin GA IV [2,3], characterized by a long fatty acyl moiety at the N-terminus; (ii) long-sequence (e.g. alamethicin) [4], with 17–21 residues; and (iii) medium-length (14–16 residues), such as among others antiamoebin [5], efrapeptin [6], and tylopeptin [7]. Despite the interesting antibiotic and antifungal properties exhibited by these last membrane-active peptides, their exact mechanism of action is still unknown.

Recently, we focused our attention on another medium-length peptaibiotic, heptaibin, which was isolated by Ishiyama *et al.* 10 years ago and found to be able to selectively inhibit the growth of Gram-positive bacteria, e.g. *Staphylococcus aureus* [8]. The heptaibin primary structure is as follows.

Ac-Phe-$(Aib)_3$-Val-Gly-Leu-$(Aib)_2$-Hyp-Gln-Aib-Hyp-Aib-Phol

where Ac is acetyl, Hyp is 4(*R*)-hydroxy-(*S*)-proline, and Phol is the 1,2-aminoalcohol L-phenylalaninol (the name of this antimicrobial peptide originates from the observation that it contains seven Aib residues).

One of the possible reasons for the lack of studies on this medium-length peptaibiotic is the intrinsic difficulty of its synthesis, mainly due to the presence in the sequence of two Aib–Hyp bonds. A characteristic feature of the Aib-Pro(Hyp) tertiary amide bonds is their acid lability [9], which makes inappropriate the use of the common Hyp side-chain protecting groups. Moreover, the relatively high tendency of the Xxx–Pro(Hyp) bonds to adopt a *cis* conformation [10] may be responsible for the easy formation of the corresponding 2,5-dioxopiperazine side product [11,12] with the resulting loss of these two residues from the peptide sequence. However, the availability of the 2-chlorotrityl resin with the 1,2-aminoalcohol anchored on it [which could be cleaved under very mild acidic conditions, namely 30% 1,1,1,3,3,3-hexafluoroisopropanol (HFIP) in CH_2Cl_2 [13]], as well as of effective coupling reagents, makes it possible to carry out this synthesis

* *Correspondence to: Marta De Zotti, Department of Chemistry, University of Padova, via Marzolo 1, 35131 Padova, Italy. E-mail: marta.dezotti@unipd.it*

a *ICB, Padova Unit, CNR, Department of Chemistry, University of Padova, via Marzolo 1, 35131 Padova, Italy*

b *Department of Biotechnology, School of Natural Sciences, Chosun University, 501-759 Gwangju, Korea*

c *Department of Bio-Materials, Research Center for Proteineous Materials, Chosun University, 501-759 Gwangju, Korea*

d *Department of Cellular and Molecular Medicine, College of Medicine, Chosun University, 501-759 Gwangju, Korea*

with reasonable yield and degree of purity. In fact, the solid-phase peptide synthesis (SPPS) of a medium-length peptaibiotic closely related to heptaibin has been recently described [14].

In this study, we performed the SPPS of heptaibin, by taking advantage of our long-term expertise in the synthesis of peptaibiotics [15]. We also carried out an in-depth conformational study on this 14-amino acid residue peptaibiotic and tested its enzymatic degradation stability, the membrane activity on small unilamellar vesicles (SUVs) of three different compositions, and the cytotoxicity on erythrocytes.

Materials and Methods

Peptide Synthesis and Characterization

Fmoc-amino acids were supplied from Novabiochem (Merck Biosciences, La Jolla, CA, USA). All other amino acid derivatives and reagents for peptide synthesis were purchased from Sigma–Aldrich (St. Louis, MO, USA). Assembly of peptides on the Advanced ChemTech (Louisville, KY, USA) 348-Ω peptide synthesizer was performed on a 0.05 mmol scale, by the FastMoc methodology as described above, starting with the Phol-substituted 2-chlorotrityl resin (Iris Biotech, Marktredwitz, Germany) (110 mg, loading 0.40 mmol/g). The peptide cleaved from the resin was filtered and collected. This step was repeated three times; then, the solution was concentrated under a flow of nitrogen. The crude peptides were purified by preparative RP-HPLC on a Vydac C_{18} column (22 × 250 mm, 10 µ, 300 Å) using a Shimadzu (Kyoto, Japan) LC-8A pump system equipped with a SPD-6A UV-detector (flow rate 15 ml/min, $\lambda = 216$ nm) and a binary elution system: A, H_2O; B, CH_3CN/H_2O (9 : 1 v/v); gradient 40–70% B in 30 min. The purified fractions were characterized by analytical RP-HPLC on a Vydac C_{18} column (4.6 × 250 mm, 5 µ, 300 Å) using a Dionex (Sunnyvale, CA, USA) P680 HPLC pump with an ASI-100 automated sample injector. The binary elution system used was as follows: A, 0.1% TFA in H_2O; B, 0.1% TFA in CH_3CN/H_2O (9 : 1 v/v); gradient 50–90% B in 30 min (flow rate 1.5 ml/min); spectrophotometric detection at $\lambda = 216$ nm.

Electrospray ionization (ESI-MS) was performed by using a PerSeptive Biosystem Mariner instrument (Framingham, MA, USA). [Hyp(Bzl)^{10,13}]-heptaibin (*m/z*): calculated for $C_{90}H_{130}N_{16}O_{19}$ $[M+H]^+$ 1739.97; found 1739.95. Heptaibin (*m/z*): calculated for $C_{76}H_{118}N_{16}O_{19}$ $[M+H]^+$ 1559.85; found 1559.86.

FT-IR Absorption Spectroscopy

The FT-IR absorption spectra were recorded at 293 K using a Perkin-Elmer model 1720X FT-IR spectrophotometer, nitrogen flushed, equipped with a sample-shuttle device, at 2 cm^{-1} nominal resolution, averaging 100 scans. Solvent (baseline) spectra were recorded under the same conditions. For spectral elaboration, the software SPECTRACALC provided by Galactic (Salem, MA, USA) was employed. Cells with path lengths of 1.0 and 10 mm (with CaF_2 windows) were used. Spectrograde deuterated chloroform (99.8%, d_2) was purchased from Merck (Darmstadt, Germany).

SUV Preparation

DOPG, DOPC, DOPE, and CL were purchased from Avanti Polar Lipids, Inc. (Alabaster, AL, USA), while CH was a Sigma-Aldrich (St. Louis, MO, USA) product. Lipid mixtures, DOPC/CH (7 : 3), DOPE/DOPG (7 : 3), or DOPG/CL (58 : 42), were dissolved in chloroform in a test tube, dried under N_2, and lyophilized overnight. The lipid film was hydrated in 4-(2-hydroxyethyl)piperazine-1-ethanesulfonic acid (Hepes) buffer (5 mM Hepes, 100 mM NaCl, pH 7.4) at room temperature for 1 h. To make SUVs, the resulting multilamellar vesicle suspension was sonicated (GEX 400 Ultrasonic Processor, Sigma) on ice until the initially cloudy lipid dispersion became translucent, then centrifuged in a Beckman ultracentrifuge at 4 °C and 150 000 × *g* for 1 h to remove titanium debris and to separate any remaining large vesicles. The supernatant was collected as SUVs with an approximate diameter of 20–30 nm as detected by light-scattering measurements. For leakage experiments requiring incorporation of CF, the lipid films were prepared, reconstituted with a solution of CF in 30 mM Hepes buffer (pH 7.4), and sonicated as described above. The excess of fluorescent dye was eliminated by gel filtration on Sephadex G-75 (Sigma). SUVs were diluted to a concentration of 0.06 mM with Hepes buffer (5 mM Hepes, 100 mM NaCl, pH 7.4). The SUVs were stored at 4 °C and used within 24 h.

Circular Dichroism Spectroscopy

The CD spectra were measured on a Jasco (Tokyo, Japan) model J-715 spectropolarimeter equipped with a Haake thermostat (Thermo Fisher Scientific, Waltham, MA, USA). Baselines were corrected by subtracting the solvent contribution. A fused quartz cell of 1.0 mm pathlength (Hellma, Mühlheim, Germany) was used. The values are expressed in terms of $[\theta]_T$, the total molar ellipticity (deg × cm^2 × $dmol^{-1}$). Spectrograde methanol 99.9% (Acros Organic, Geel, Belgium) was used as solvent. The CD measurements in membranes were carried out with a fused quartz cell of 0.5-mm pathlength (Hellma, Mühlheim, Germany).

Nuclear Magnetic Resonance Spectroscopy

Samples for NMR spectroscopy were dissolved in water (9 : 1 H_2O/D_2O) containing SDS-d_{25} (100 mM) or in MeOH-d_3 solution (peptide concentrations: 2 and 1 mM, respectively). The pH of the SDS-containing solution was adjusted at 5.53 by adding 5 µl of 6 M HCl and the spectra were recorded at 313 K. All NMR experiments were performed on a Bruker AVANCE DMX-600 spectrometer using the TOPSPIN software package. Presaturation of the H_2O solvent signal was obtained using a WATERGATE gradient program. All homonuclear spectra were acquired by collecting 512 experiments, each one consisting of 64–80 scans and 2 K data points. The spin systems of protein amino acid residues were identified using standard DQF-COSY [16] and CLEAN-TOCSY [17,18] spectra. In the latter case, the spin-lock pulse sequence was 70 ms long. The assignment of the two methyl groups belonging to the same Aib residue was obtained by means of $^1H-^{13}C$ 2D correlation spectra. To optimize the digital resolution in the carbon dimension, heteronuclear multiple quantum coherence (HMQC [19]) and heteronuclear multiple bond coherence (HMBC [20]) experiments were acquired using selective excitation by means of Gaussian-shaped pulses with 1% truncation [21,22].

The C^{β}-selective HMQC experiments with gradient coherence selection [23] were recorded with 320 t_1 increments, of 300 scans and 2 K points each [19]. A spectral width of 16 ppm centered at 22 ppm in F1 was used, yielding a digital resolution of 2.36 Hz/pt prior to zero filling. HMBC experiments with selective excitation in the CO region were performed using a long-range coupling constant of 7.5 Hz, a spectral width in F1 of 15 ppm centered at

176 ppm, 250 t_1 experiments of 640 scans, and 4 K points in F2. The digital resolution in F1, prior to zero filling, was 2.2 Hz/pt. NOESY experiments were used for sequence-specific assignment. To avoid the problem of spin diffusion, the build-up curve of the volumes of NOE cross-peaks as a function of the mixing time (50–500 ms) was determined first (data not shown). The mixing time of the NOESY experiment used for interproton distance determination was 150 ms, that is, in the linear part of the NOE build-up curve. Interproton distances were obtained by integration of the NOESY spectrum using the SPARKY 3.111 software package. The calibration was based on the average of the integration values of the cross peaks due to the interactions between the two β-geminal protons and between the two δ-geminal protons of the Hyp[10] and Hyp[13] side-chain residues, set to a distance of 1.78 Å.

Distance geometry and MD calculations were carried out using the random-simulated annealing (rSA) protocol of the XPLOR-NIH 2.9.6 program [24]. For distances involving equivalent or nonstereo-assigned protons, r^{-6} averaging was used. The MD calculations involved a minimization stage of 100 cycles, followed by SA and refinement stages. The SA consisted of 30 ps of dynamics at 1500 K (10 000 cycles, in 3 fs steps) and of 30 ps of cooling from 1500 to 100 K in 50 K decrements (15 000 cycles, in 2 fs steps). The SA procedure, in which the weights of NOE and nonbonded terms were gradually increased, was followed by 200 cycles of energy minimization. In the SA refinement stage, the system was cooled from 1000 to 100 K in 50 K decrements (20 000 cycles, in 1 fs step). Finally, the calculations were completed with 200 cycles of energy minimization using a NOE force constant of 50 kcal/mol. The generated structures were visualized using the MOLMOL [25] (version 2K.2) program.

Proteolytic Stability

The proteolytic stability of synthetic heptaibin was assessed using pronase E and chymotrypsin (Sigma–Aldrich). The peptide (0.125 mg) was dissolved in the minimum amount (5 µl) of DMSO (dimethylsulfoxide) and then diluted (final volume: 50 µl) with the appropriate buffer (2-amino-2-hydroxymethyl-propane-1,3-diol (Tris)·HCl 20 mM, containing 20 mM $CaCl_2$ pH 7.6 for pronase E; Tris·HCl 50 mM, pH 7.8 for chymotrypsin). Then, it was incubated with and without the enzyme solution (1.25 µg of enzyme in 150 µl buffer) at 37 °C for 12 h. After the workup procedures, the samples were analyzed by RP-HPLC as described in the 'peptide synthesis and characterization' experimental section. A peptide not resistant to pronase E and chymotripsin was used as a positive test.

Membrane Activity

Synthetic heptaibin-induced leakage from SUVs of different composition was measured at 293 K using the CF-entrapped vesicle technique [26] and a Perkin-Elmer model MPF-66 spectrofluorimeter. The SUVs composition used were (i) mammalian erythrocytes mimic: DOPC/Ch 7 : 3; (ii) Gram-negative bacteria mimic: DOPE/DOPG 7 : 3; (iii) Gram-positive bacteria mimic: DOPG/CL 58 : 42. SUVs were prepared as described above. The phospholipid concentration was kept constant (0.06 mM) and increasing [peptide]/[lipid] molar ratios (R^{-1}) were obtained by adding aliquots of MeOH solutions of peptides, keeping the final MeOH concentration below 5% by volume. After rapid and vigorous stirring, the time course of fluorescence change corresponding to CF escape was recorded at 520 nm (6-nm band pass) with λ_{exc} 488 nm (3-nm band pass). The percentage of released CF at time t was determined as $(F_t - F_0)/(F_T - F_0) \times 100$, with F_0 is the fluorescence intensity of vesicles in the absence of peptide, F_t the fluorescence intensity of vesicles at time t in the presence of peptide, and F_T the total fluorescence intensity determined by disrupting the vesicles by addition of 50 µL of a Triton X-100 solution. The kinetics experiments were stopped at 20 min. We used trichogin GA IV [2,3], a well-known membrane active peptaibiotic, as a positive test.

Hemolytic Activity

The hemolytic activity of synthetic heptaibin was determined using human red blood cells (hRBCs) from healthy donors that were collected on heparin. Fresh hRBCs were washed three times in PBS by centrifugation for 10 min at 800 g and resuspension in PBS. The peptide was dissolved in the minimum amount of DMSO, diluted with PBS to the desired concentration (in the range 10–500 µg/ml) and then added to 100 µl of stock hRBCs suspended in PBS (final hRBCs concentration: 8%, v/v). The maximum amount of DMSO in each solution was 1.4%. The samples were incubated with agitation for 1 h at 37 °C and centrifuged at 800 g for 10 min. The absorbance of the supernatant was measured at 414 nm. Controls for zero hemolysis (blank) and 100% hemolysis consisted of hRBCs suspended in PBS and 1% Triton X-100, respectively. The percentage hemolysis was calculated using the following equation: % hemolysis = $[(A_{414\ nm}$ with peptide solution $- A_{414\ nm}$ in PBS)/($A_{414\ nm}$ with 0.1% Triton X-100 $- A_{414\ nm}$ in PBS)$] \times 100$. Each measurement was made in triplicate [27]. The hemolytic peptide melittin was synthesized in the Chosun University laboratories.

Results and Discussion

In this work, we synthesized by automatic SPPS natural heptaibin, an N^{α}-blocked peptide alcohol, and an analog where the hydroxyl function of each of the two Hyp residues at positions 10 and 13 is benzylated. These difficult syntheses [14] were performed on a Phol-substituted 2-chlorotrityl resin with a checked loading of 0.4 mmol/g.

Because of the presence of two highly acid-labile Aib–Hyp bonds [9] in the sequence, we first decided to protect the side-chain Hyp[10,13] hydroxyl functions as benzyl ethers and to leave the Gln[11] primary amide group unprotected. The total syntheses were achieved by using the very efficient HATU [2-(1*H*-7-aza-1,2,3-benzotriazol-1-yl)-1,1,3,3-tetramethyl uronium hexafluorophosphate] [28] C-activation procedure, which *inter alia* proved to be essential to overcome the problems arising from the poorly reactive amino functionality of the (50% of the total) Aib residues, three of them positioned consecutively in the sequence. In this connection, it is worth pointing out that the HATU coupling additive by itself [29], as opposed to *N*-[3-(dimethylamino)-propyl]-*N'*-ethylcarbodiimide (EDC)/1-hydroxy-1,2,3-benzotriazole (HOBt) [30] or EDC/7-aza-1-hydroxy-1,2,3-benzotriazole (HOAt) [28], does not fully prevent nitrile formation from the Gln side chain (this positive effect seems to be generated by the presence of HOAt or HOBt) [29]. Indeed, about 5% of the nitrile-containing product was seen in our ESI-MS spectroscopic analysis using HATU alone. The coupling reactions, carried out by the use of a threefold excess of the Fmoc (fluorenyl-9-methyloxycarbonyl)-protected amino acid and HATU, in the presence of a sevenfold excess of N,N-diisopropylethylamine, for 60 min were doubled when performed on an N-terminated Aib peptide or when Aib is the incoming residue.

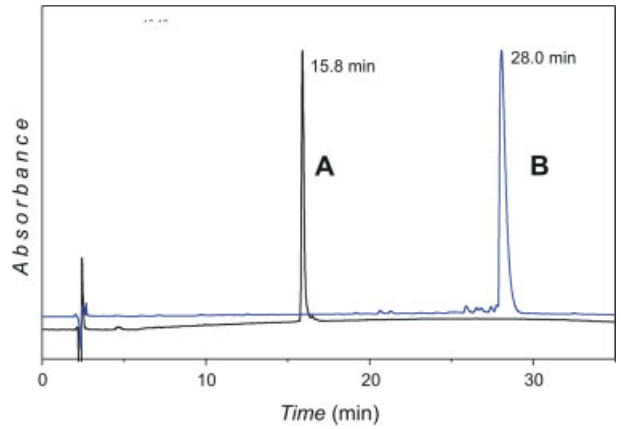

Figure 1. Analytical RP-HPLC profiles obtained for the purified synthetic heptaibin (A) and its [Hyp(Bzl)^{10,13}] analog (B). This figure is available in colour online at wileyonlinelibrary.com/journal/jpepsci.

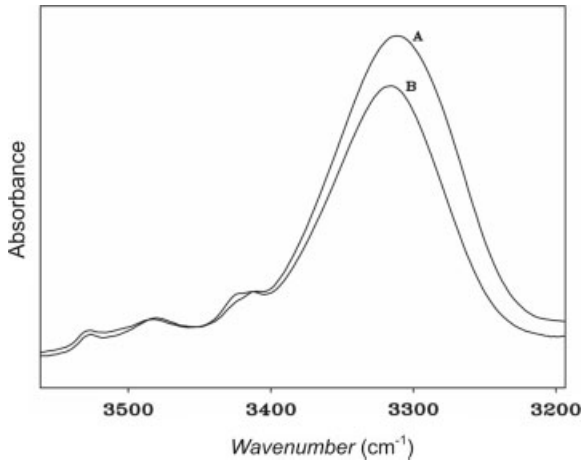

Figure 2. FT-IR absorption spectra of the [Hyp(Bzl)^{10,13}] heptaibin analog in $CDCl_3$ solution. Peptide concentrations: 1 mM (A) and 0.1 mM (B).

Removal of the Fmoc N$^{\alpha}$-protection was performed by treatment with 20% piperidine in *N*,*N*-dimethylformamide. Specific attention was devoted to the deprotection of the Aib^{12} and Aib^{9} residues to avoid the easy 2,5-dioxopiperazine formation at the level of the free N-terminal -H-Aib-Hyp-dipeptide sequence. In particular, the Fmoc protection was removed from Aib^{12} and Aib^{9} in two steps of 5 min each, instead of using the standard procedure which requires two steps of 10 and 15 min each.

Final on-resin N$^{\alpha}$-acetylation was achieved using AcOH preactivated with EDC/HOAt in the presence of *N*-methylmorpholine. Cleavage of the peptide from the 2-chlorotrityl resin was performed by repeated treatments with 30% HFIP in distilled CH_2Cl_2 (45 min each). The [Hyp(Bzl)^{10,13}]-heptaibin peptide was purified by HPLC [in the absence of trifluoroacetic acid (TFA), a potential cleaving agent for the Aib–Hyp bonds] and characterized by ESI-MS and ^{1}H-NMR techniques (see below). However, any subsequent, small-scale, attempt to remove the two Hyp O-benzyl protections, using catalytic (H_2/Pd) hydrogenolysis, was unsuccessful, providing in all cases untreatable mixtures of a number of side products. At this point, unfortunately, we were forced to conclude that this route is unsuitable for the total synthesis of natural heptaibin.

In our second synthetic route, we left both the two Hyp and the single Gln side chains unprotected. All of the various steps were conducted as described above for the preparation of [Hyp(Bzl)^{10,13}]-heptaibin, with the single exception of the activation of the Gln α-carboxylic function, which was carried out using HATU/HOAt (no evidence of nitrile formation was found in this case). However, to reduce the potential impact of the reactivity of the two Hyp hydroxyls (although it is known that these groups are less nucleophilic than the α-NH_2 function) we decided to limit the excess of any acylating reagent to ≈10%. We find that the HPLC profile of the final crude heptaibin is not significantly deteriorated as compared to that of its [Hyp(Bzl)^{10,13}] analog. This finding indicates that the Hyp hydroxyl groups do not undergo any marked acylation under the experimental conditions used. Again, the final, 98% pure, heptaibin product (obtained in a 20% yield) was characterized by ESI-MS and ^{1}H-NMR (see below). Interestingly, the SPPS of the strictly related peptaibiotic bergofungin D carried out by a procedure different from that reported here for heptaibin was achieved in only 11% isolated yield [14]. The RP-HPLC profiles of the purified, synthetic heptaibin and its [Hyp(Bzl)^{10,13}] analog are reported in Figure 1.

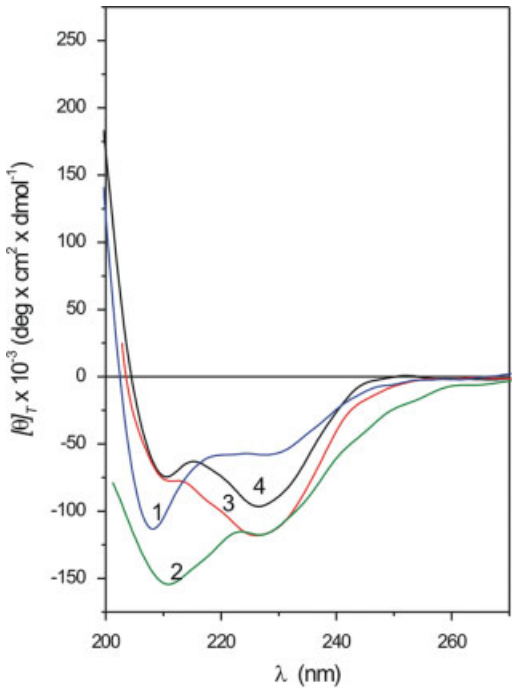

Figure 3. CD spectra of synthetic heptaibin in MeOH (1) and in the DOPC/CH (2), DOPE/DOPG (3), and DOPG/CL (4) model membranes. Peptide concentrations: 0.1 mM in MeOH and 0.05 mM in liposomes.

Conformational Analysis

A detailed analysis of the conformational preferences of the synthetic heptaibin and its [Hyp(Bzl)^{10,13}] analog synthesized in this work was performed using FT-IR absorption, CD, and 2D-NMR spectroscopy in different solvents and environments.

As heptaibin is not soluble in $CDCl_3$, we carried out the FT-IR absorption study of the [Hyp(Bzl)^{10,13}] analog only. In the conformationally informative 3550–3200 cm^{-1} region at 1.0 mM concentration, the spectrum is dominated by an intense absorption at 3312 cm^{-1}, assigned to the N–H stretching mode of H-bonded peptide groups [31–33] (Figure 2). An additional, very weak and broad band is visible at about 3420 cm^{-1}, attributed to free (solvated) amide/peptide groups. The even smaller bands

Journal of PeptideScience

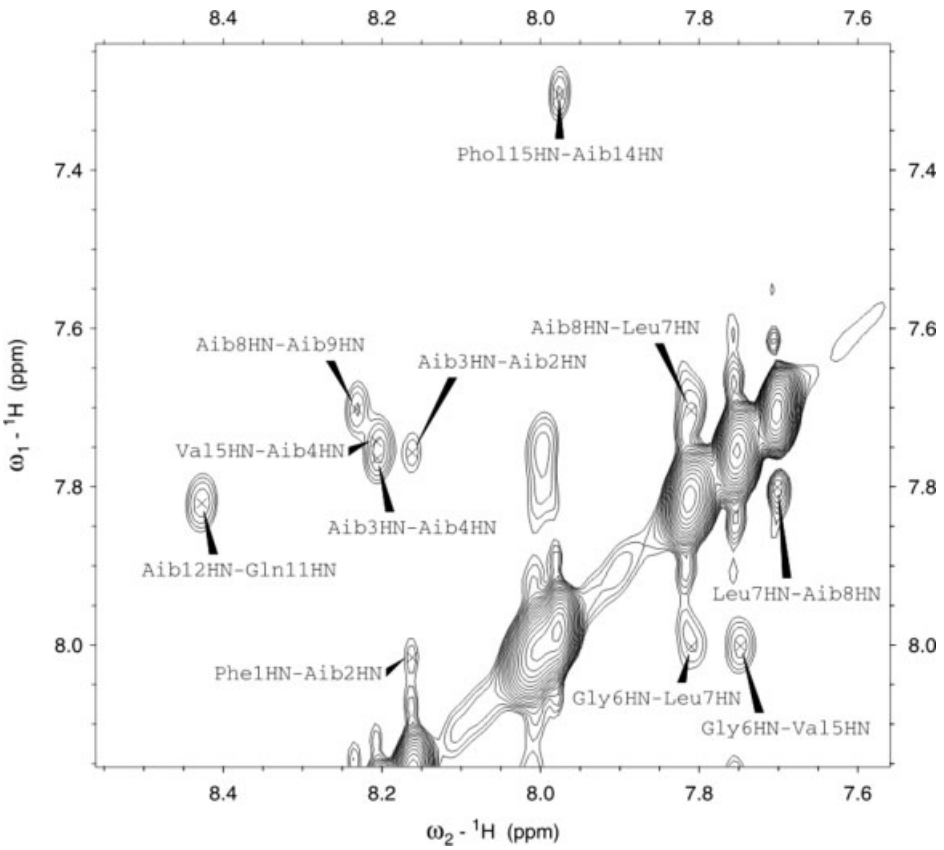

Figure 4. Amide NH proton region of the NOESY spectrum of synthetic heptaibin in water (9 : 1 H_2O/D_2O) containing SDS-d_{25} (100 mM). Peptide concentration: 2.0 mM.

above 3450 cm^{-1} are related to O–H stretching modes of the C-terminal aminoalcohol [31]. Only a modest dilution effect is seen in the spectrum of the peptide between 1.0 and 0.1 mM concentration (Figure 2). This difference is probably associated with a slight tendency of this analog to aggregate. Therefore, the observed spectrum at the lowest concentration examined should be interpreted as arising almost exclusively from intramolecular C═O···H–N interactions. We conclude that this FT-IR absorption spectrum is consistent with the hypothesis that in $CDCl_3$, a solvent of low polarity, the preferred conformation of heptaibin, rich in the helix-supporting Aib residue [34–36], would be highly folded and extensively stabilized by H-bonds.

The CD spectra of synthetic heptaibin were recorded in a set of different environments, a polar solvent (MeOH, methanol) and three different types of model membranes: 1,2-dioleoyl-*sn*-glycero-3-phosphocholine (DOPC)/cholesterol(CH) 7 : 3; 1,2-dioleoyl-*sn*-glycero-3-phosphoethanolamine (DOPE)/1,2-dioleoyl-*sn*-glycero-3-phospho-(1′-*rac*-glycerol) (DOPG) 7 : 3; and DOPG/1′,3′-bis[1,2-dioleoyl-*sn*-glycero-3-phospho]-*sn*-glycerol (sodium salt) /cardiolipin (CL) 58 : 42. Each of the curves exhibits two negative Cotton effects of moderate intensities, located near 227 nm ($n \rightarrow \pi^*$ transition of the peptide chromophore [37]) and 210 nm (parallel component of the split peptide $\pi \rightarrow \pi^*$ transition) (Figure 3). This overall pattern is reminiscent of that typically shown by significantly developed, right-handed, helical structures [37,38]. The value of the $[\theta]_{222}/[\theta]_{208}$ ellipticity ratio (R) in MeOH (0.60) is indicative of a largely mixed 3_{10}-/α-helix conformation [38–40]. The shape of the CD curve does not change appreciably in the zwitter-ionic (DOPC/CH) model membrane. However, the relative intensities of the two negative ellipticity maxima in the two negatively charged (DOPE/DOPG and DOPG/CL) model membranes were found to be the opposite to that observed in DOPC/CH. It is reasonable to conclude that only the DOPE/DOPG and DOPG/CL molecules [41] are able to interact with and slightly perturb the helical structure occurring in the absence of lipids. It is difficult to attribute the observed CD effect to a single parameter as it is known that the $n \rightarrow \pi^*$ dichroic band intensity may be altered by a variety of factors (length or distortion of the helix, percentage of 3_{10}- *versus* α-helix, shortening of the intramolecular C═O···H–N H-bonds, peptide self-association) [42–46].

The NMR analysis is expected to offer a more detailed view of the conformation of the peptaibiotic at the local level. The 2D-NMR spectra of synthetic heptaibin were first acquired in MeOH solution. The assignments of the proton resonances, obtained following the Wüthrich procedure [47], are in agreement with those of the natural peptaibiotic in the same solvent [8]. Our ROESY spectrum exhibits all $NH_i \rightarrow NH_{i+1}$ sequential cross peaks (except that at the N-terminus, between the Phe^1 and Aib^2 NH protons) and one $NH_i \rightarrow NH_{i+2}$ C-terminal cross peak (between the Aib^{12} and Aib^{14} NH protons), characteristic of the presence of a helical structure (Supporting Information). Although two Hyp residues characterize the heptaibin sequence, no evidence for a *cis* conformation at any of the tertiary amide Xxx–Hyp bonds was found, most probably because in both cases the Xxx residue is the sterically hindered Aib [35]. In the fingerprint region (Supporting Information), a number of C^α $H_i \rightarrow NH_{i+3}$ cross peaks are seen, along with few C^α $H_i \rightarrow NH_{i+4}$ and C^α $H_i \rightarrow NH_{i+2}$ cross peaks. Taken together, the present findings, which favor the occurrence

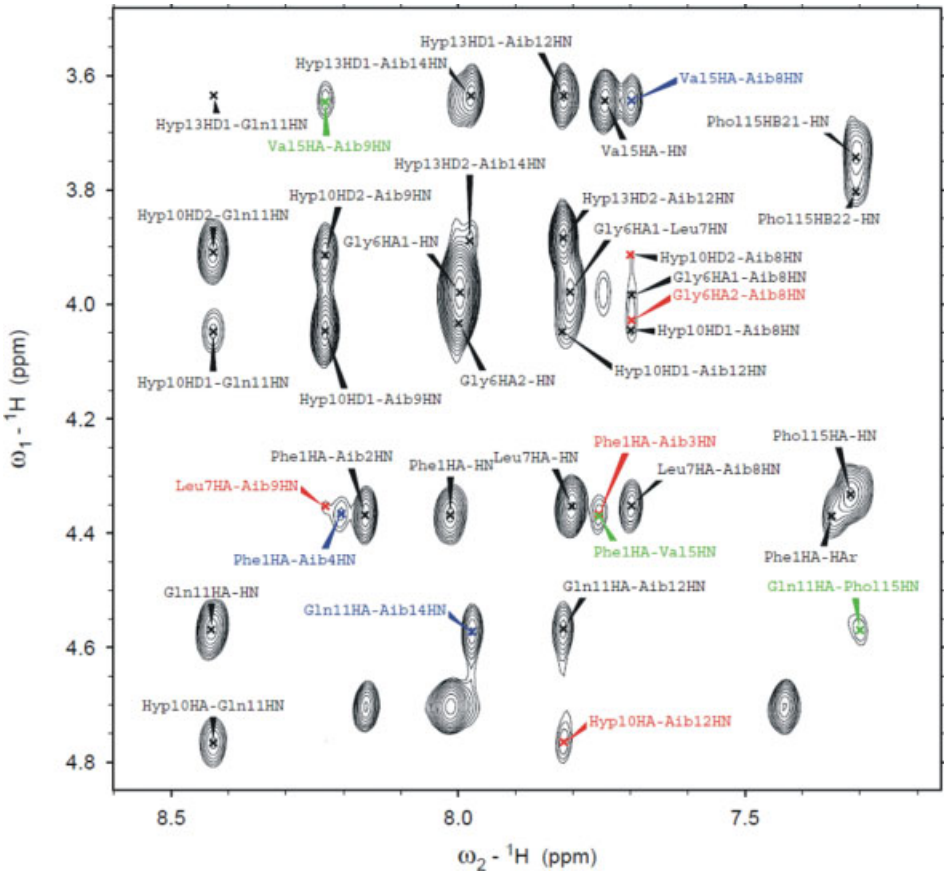

Figure 5. Fingerprint region of the NOESY spectrum of synthetic heptaibin in water (9 : 1 H_2O/D_2O) containing SDS-d_{25} (100 mM). Peptide concentration: 2.0 mM. The $C^{\alpha}H_i \rightarrow NH_{i+2}$, $C^{\alpha}H_i \rightarrow NH_{i+3}$, and $C^{\alpha}H_i \rightarrow NH_{i+4}$ cross-peaks are highlighted in red, blue, and green, respectively.

of a mixed 3_{10}-/α-helix conformation for this peptaibiotic in MeOH, nicely confirm our CD results in the same solvent discussed above.

To better understand the conformational preferences of heptaibin in an environment mimetic of negatively charged membranes, we recorded the 2D-NMR spectra in a SDS aqueous mixture. Moreover, to complete the assignments of the resonances of the Aib residues, the hetero-correlated $^{13}C-^{1}H$ C═O selective HMBC and C^{β} selective HMQC 2D-NMR spectra were analyzed. In particular, for the configurational assignment of the two prochiral Aib methyl groups we used a selective HMQC experiment centered in the $^{\beta}$ CH_3 region of the ^{13}C spectrum (20–40 ppm region) [48].

In the NOESY spectrum, all $NH_i \rightarrow NH_{i+1}$ sequential cross peaks are seen (Figure 4), which is a clear indication of a fully developed helical structure. Again, in the fingerprint region (Figure 5) the 3_{10}-helix C^{α} $H_i \rightarrow NH_{i+2}$ cross peaks concomitantly occur with the α-helix C^{α} $H_i \rightarrow NH_{i+4}$ cross peaks. The former are extensively recognized in the N-terminal segment. A summary of the significant inter-residue cross peaks is given in Figure 6.

The NOESY spectrum with a mixing time of 150 ms was chosen as the most suitable to perform the restrained molecular dynamics (MD) calculations. A total of 86 inter-proton distance restraints were derived (Table 1) and used in the random simulating annealing protocol. Out of the 150 3d-structures generated, 127 had violations to the NOE restraints lower than 0.5 Å. The 54 structures with a total energy <147 kcal/mol (Table 2) were selected. Their superposition is shown in Figure 7. All these structures converge to a mixed 3_{10}-/α-helical conformation, with a modest distortion at the Hyp[10] level (average kink angle: $25^{\circ} \pm 3^{\circ}$).

The side chains of the three hydrophilic residues (Hyp[10], Gln[11], and Hyp[13]), which lie on the same face of the helix (Figure 8), provide an amphiphilic character to the overall structure. Moreover, also Gly[6], the less hydrophobic residue in the N-terminal part of the sequence, is located on the hydrophilic face, thus reinforcing the global amphiphilicity of the helix.

Protease Resistance

Proteolytic degradation of a bioactive peptide may reduce its duration of action and change its pharmacological profile. For this reason, we tested the biostability of synthetic heptaibin to determine whether peptide bonds involving the Phe residue at the N-terminus or other amino acids are enzymatically hydrolyzed. Pronase E and α-chymotrypsin were used to evaluate the *in vitro* resistance. Pronase E is a metalloprotease isolated from *Streptomyces griseus* which is not selective as it can cleave backbone peptide bonds at many different sites. Conversely, chymotrypsin, a member of the Ser-protease class, is an endopeptidase that selectively cleaves peptide bonds on the C-terminal side of aromatic (e.g. Phe) or aliphatic and largely hydrophobic (e.g. Leu) residues.

The process was followed by the use of RP-HPLC. As a typical example, the results in the presence of pronase E are shown in Figure 9. Heptaibin was found intact after the pronase E (and the α-chymotrypsin as well) degradation assay, presumably due to the high content (50%) of the noncoded C^{α}-tetrasubstituted (bulky) α-amino acid Aib. In a few previous papers the authors have already reported a significant protection for Aib-containing

Journal of PeptideScience

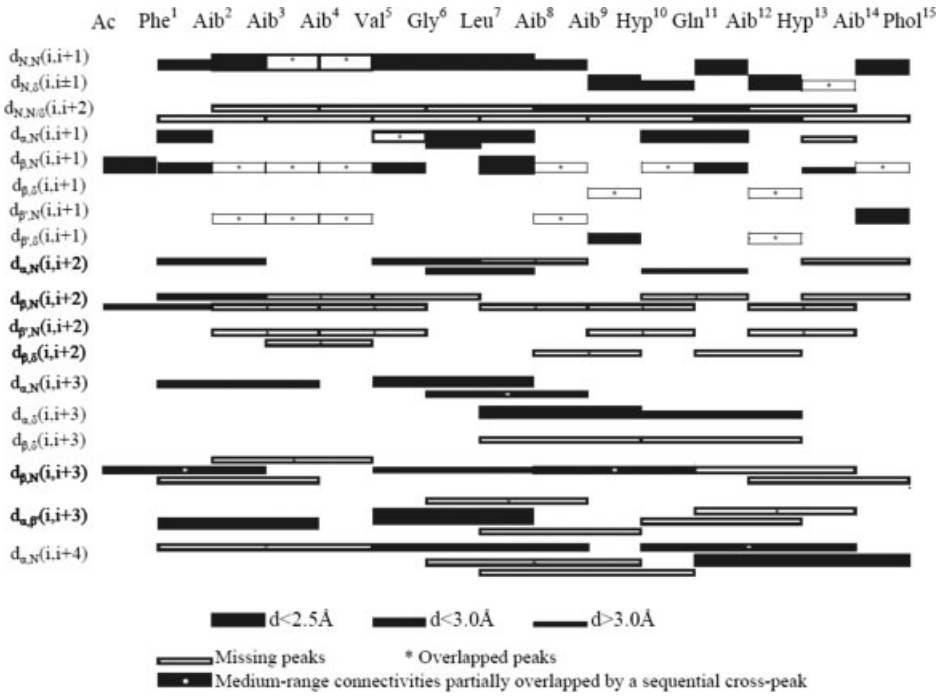

Figure 6. Summary of the significant inter-residue NOESY cross peaks for synthetic heptaibin in water (9 : 1 H_2O/D_2O) containing SDS-d_{25} (100 mM). Peptide concentration: 2.0 mM.

Table 1. NOE constraints, deviations from idealized geometry, and mean energies for the NMR-based structures of synthetic heptaibin in water (9 : 1 H_2O/D_2O) containing SDS-d_{25} (100 mM)

Number of NOEs	
Total	86
Intraresidue	25
Sequential	37
$i, i+n, n = 2, 3, 4$	24
Mean rmsd[a] from ideality of accepted structures	
Bonds (Å)	0.00627
Angles (°)	0.9131
Improper (°)	47.029
NOEs (Å)	0.1289
Mean energies (kcal/mol) of accepted structures	
$E_{overall}$	145.3
E_{bond}	9.134
E_{angle}	53.19
E_{NOE}	67.31

[a] Root-mean-square deviation.

Table 2. Average values (°) of torsion angles ϕ_m and ψ_m and the relative standard deviations resulting from the 54 calculated structures (energy <147 kcal/mol) of synthetic heptaibin in water (9 : 1 H_2O/D_2O) containing SDS-d_{25} (100 mM)

Residue	ϕ_m	$\Delta\phi$	ψ_m	$\Delta\psi$
Phe[1]	–	–	−59.5	±1.1
Aib[2]	−59.5	±1.8	−15.4	±1.2
Aib[3]	−80.9	±1.9	−34.0	±6.8
Aib[4]	−65.7	±6.2	−41.4	±9.3
Val[5]	−61.4	±3.6	−32.7	±3.2
Gly[6]	−57.0	±3.2	−35.5	±4.9
Leu[7]	−86.9	±3.2	−28.0	±1.4
Aib[8]	−78.5	±1.1	−37.1	±1.9
Aib[9]	−56.0	±1.6	−39.8	±0.9
Hyp[10]	−77.4	±0.6	−1.0	±0.8
Gln[11]	−105.8	±2.1	−10.0	±0.9
Aib[12]	−62.9	±1.8	−33.5	±1.0
Hyp[13]	−85.5	±0.7	−53.7	±1.0
Aib[14]	−66.1	±2.6	−39.8	±1.9
Phol[15]	−95.7	±4.6	–	–

peptides from being proteolytically digested [49–52]. However, only in two cases [50,52] the potential contribution of Aib-induced helical structure [34–36] in reducing protease recognition was mentioned.

Membrane Activity

The membrane permeability properties of synthetic heptaibin were tested in comparison with our typical reference compound for this type of study, i.e. the lipopeptaibol trichogin GA IV [2,3], by measuring the induced leakage of 5(6)-carboxyfluorescein (CF) entrapped in SUVs (Figure 10). For this investigation, the three different types of model membranes mentioned above were exploited: the overall neutral, zwitter-ionic DOPC/CH (mammalian erythrocytes mimic), the overall negatively charged DOPE/DOPG [Gram-negative (*E. coli*) bacteria mimic], and the negatively charged DOPG/CL [Gram-positive (*S. aureus*) bacteria mimic].

It is worth noting that the permeability effect of trichogin GA IV is quite remarkable in the presence of all of the three types of model membranes, although slightly less efficient in the presence of that mimicking the surface of Gram-negative bacteria. Conversely,

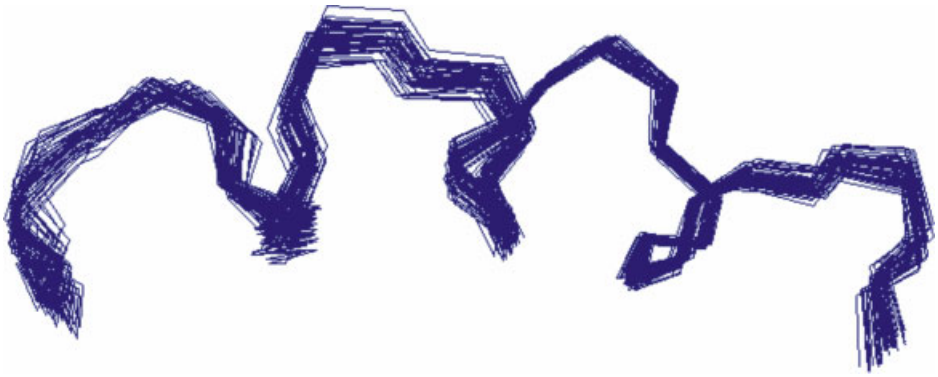

Figure 7. Backbone representation of the 54 3D-structures with energy <147 kcal/mol resulting from the MD calculations of synthetic heptaibin with the backbone atoms superimposed, consistent with the NMR-distances restraints. This figure is available in colour online at wileyonlinelibrary.com/journal/jpepsci.

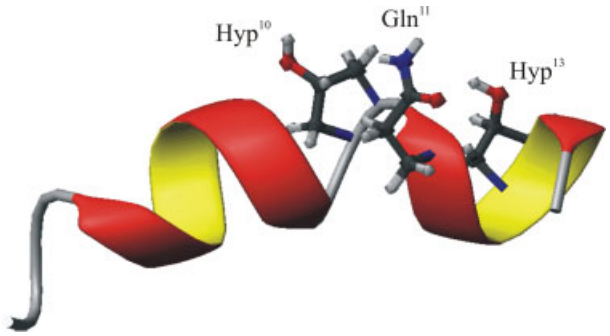

Figure 8. Ribbon representation of the lowest energy (143 kcal/mol) 3D-structure obtained for synthetic heptaibin. The hydrophilic Hyp^{10}, Gln^{11}, and Hyp^{13} residues are labeled.

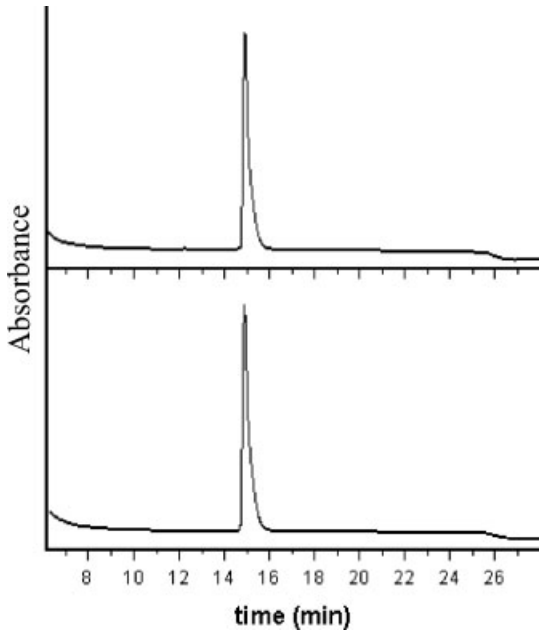

Figure 9. RP-HPLC profiles obtained for synthetic heptaibin after 12-h incubation in Tris buffer (upper part) and in the presence of the proteolytic enzyme pronase E (lower part).

synthetic heptaibin is a much more membrane-selective peptaibiotic in that it is able to disrupt exclusively the DOPG/CL SUV which mimicks the surface of Gram-positive (*S. aureus*) bacteria. These results complement nicely the antimicrobial activity data reported for natural heptaibin [8]. Interestingly, a parallel trend stands out clearly between our CD findings and the ability of heptaibin to permeate the three types of SUVs. It is evident that only the negatively charged SUVs induce some (although not dramatic) sort of 3D-structural reorganization in the heptaibin molecules, which may contribute to the intriguing membrane selectivity exhibited by this medium-length peptaibiotic.

Hemolytic Activity

To determine the cytotoxicity of synthetic heptaibin against hRBCs, the hemolysis percentage was measured after 1 h of incubation in phosphate buffered saline (PBS). We find that an extremely low (<2%) level of hemolysis is caused by this peptaibiotic at concentrations below 250 μg/ml. Conversely, the antimicrobial peptide melittin, used as a standard in our test, shows a strong hemolytic activity above 20 μg/ml.

Conclusion

In this article, we reported a valuable protocol for the unprecedented, difficult SPPS of the medium length (14-mer) peptaibiotic heptaibin. Serious difficulties arise from (i) the homo-tripeptide sequence near the N-terminus based on the sterically hindered, C^{α}-tetrasubstituted residue Aib and (ii) the C-terminal segment characterized by the -$(Aib)_2$-Hyp-Gln-Aib-Hyp-Aib- sequence. A combination of unprotected hydroxyl and primary amide side chains, and exploitation of the Phol-substituted 2-chlorotrityl resin and the effective HATU coupling reagent allowed us to obtain heptaibin in an acceptable yield after HPLC purification.

Our detailed conformational analysis in solution showed that heptaibin is folded in a right-handed, largely mixed 3_{10}-/α-helical conformation throughout the length of the sequence. Moreover, the MD calculations provided evidence for a bending at the Hyp^{10} level, with an average angle between the preceding and following helical axes of $25 \pm 3^{\circ}$. This value is close to those found in the X-ray diffraction structures of the related, long peptaibiotic alamethicin [53] and a spin-labeled analog [54] at the Pro^{14} level. The bending of helices is a common feature of antibiotic peptide (in particular, peptaibiotic) 3D-structures [54]. This effect has been hypothesized to be related to the relative orientation of the hydrophilic/hydrophobic amino acid side chains

Journal of PeptideScience

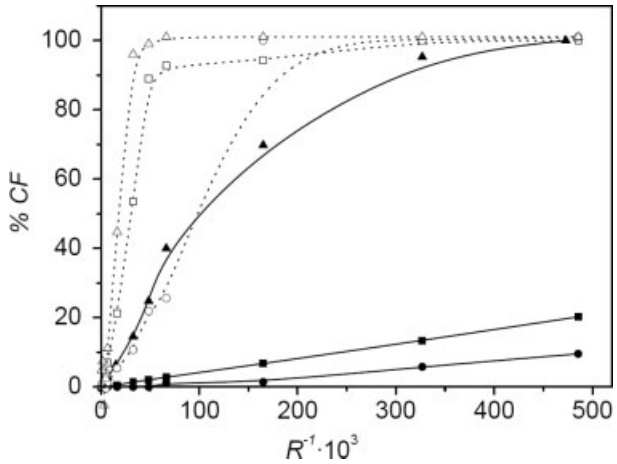

Figure 10. Synthetic heptaibin-induced (solid-lines) CF leakage from SUVs of different composition for varying ratios R^{-1} = [peptide]/[lipid]. -■- DOPC/CH, mammalian erythrocytes mimic; -●- DOPE/DOPG, Gram-negative bacteria mimic; -▲- DOPG/CL, Gram-positive bacteria mimic. Same (open) symbols for trichogin GA IV (dashed lines).

(i.e. to the peptide amphiphilic character), mode of insertion of the peptide into the bilayers, channel self-assembly, and voltage gating, or to be required to accommodate the motions of the two leaflets of the bilayer [54]. The first detailed analyses of the effect of helix kink on the activity and selectivity of an antimicrobial peptide have been recently reported [55].

Moreover, the occurrence of a large number of sterically demanding Aib residues in the sequence of heptaibin is probably the factor responsible for its impressive resistance to enzymatic degradation. Not surprisingly, our extensive leakage experiments pointed out that heptaibin, known to be active against Gram-positive bacteria only [8], is able to disrupt exclusively the overall negatively charged SUVs mimicking precisely the surface of that specific microbial class. Therefore, the interesting, selective biological properties of this peptaibiotic are confirmed by our present preliminary biophysics investigation. The availability of an efficient strategy for the preparation of heptaibin, its proteolytic enzyme stability, the selectivity against specific model membrane types, and the lack of hemolytic activity are all factors which provided useful hints for the planning of novel analogs of this peptaibiotic that we are currently using as a promising scaffold in our synthetic efforts.

Acknowledgement

This work was supported by a grant from PRIN 2008 of the Italian Ministry of University and Research (MIUR).

Supporting information

Supporting information may be found in the online version of this article.

References

1 Toniolo C, Brückner H. *Peptaibiotics*. Wiley-VCD/VHCA: Weinheim/Zürich, 2009.
2 Peggion C, Formaggio F, Crisma M, Epand RF, Epand RM, Toniolo C. Trichogin: a paradigm for lipopeptaibols. *J. Pept. Sci.* 2003; **9**: 679–689.
3 Toniolo C, Crisma M, Formaggio F, Peggion C, Epand RF, Epand RM. Lipopeptaibols, a novel family of membrane active, antimicrobial peptides. *Cell. Mol. Life Sci.* 2001; **58**: 1179–1188.
4 Leitgeb B, Szekeres A, Manczinger L, Vagvölgyi C, Kredics L. The history of alamethicin: a review of the most extensively studied peptaibol. *Chem. Biodivers.* 2007; **4**: 1027–1051.
5 Shenkarev ZO, Paramonov AS, Nadezhdin KD, Bocharov EV, Kudelina IA, Skladnev DA, Tagaev AA, Yakimenko ZA, Ovchinnikova TV, Arseniev AS. Antiamoebin I in methanol solution: rapid exchange between right-handed and left-handed 3_{10}-helical conformations. *Chem. Biodivers.* 2007; **4**: 1219–1242.
6 Jost M, Wegelt S, Huber T, Majer Z, Greie J-C, Altendorf K, Sewald N. Synthesis, and structural and biological studies of efrapeptin C analogues. *Chem. Biodivers.* 2007; **4**: 1170–1182.
7 Gobbo M, Poloni C, De Zotti M, Peggion C, Biondi B, Ballano G, Formaggio F, Toniolo C. Synthesis, preferred conformation, and membrane activity of medium-length peptaibiotics: tylopeptin B. *Chem. Biol. Drug Des.* 2010; **75**: 169–181.
8 Ishiyama D, Satou T, Senda H, Fujimaki T, Honda R, Kanazawa S. Heptaibin, a novel antifungal peptaibol antibiotic from *Emericellopsis* sp. BAUA8289. *J. Antibiot.* 2000; **53**: 728–732.
9 Theis C, Degenkolb T, Brückner H. Studies on the selective trifluoroacetolytic scission of native peptaibols and model peptides using HPLC and ESI-CID-MS. *Chem. Biodivers.* 2008; **5**: 2337–2355.
10 MacArthur MW, Thornton JM. Influence of proline residues on protein conformation. *J. Mol. Biol.* 1991; **218**: 397–412.
11 Gerig JT, Mc Leod RS. Attempted synthesis of 2-methylalanyl-L-prolyl-L-tryptophan. An unexpected result. *J. Org. Chem.* 1976; **41**: 1653–1655.
12 Brückner H, Currle M. In *Second Forum Peptides*. Aubry A, Marraud M, Vitoux B (eds). Libbey: London, 1989; 251–255.
13 Bolhagen R, Schmiedberger M, Barlos K, Grell E. A new reagent for the cleavage of fully protected peptides synthesized on 2-chlorotrityl resin. *Chem. Commun.* 1994; 2559–2560.
14 Hjørringgaard CU, Pedersen JM, Vosegaard T, Nielsen NC, Skrydstrup T. An automatic solid-phase synthesis of peptaibols. *J. Org. Chem.* 2009; **74**: 1329–1332.
15 Formaggio F, Broxterman QB, Toniolo C. In *Houben-Weyl: Methods of Organic Chemistry, Synthesis of Peptides and Peptidomimetics*. Vol. E22c, Goodman M, Felix A, Moroder L, Toniolo C (eds). Thieme: Stuttgart, 2003; 292–310.
16 Rance M, Sørensen OW, Bodenhausen G, Wagner G, Ernst RR, Wüthrich K. Improved spectral resolution in COSY ^{1}H NMR spectra of proteins via double quantum filtering. *Biochem. Biophys. Res. Commun.* 1983; **117**: 479–485.
17 Bax A, Davis DG. MLEV-17-based two-dimensional homonuclear magnetization transfer spectroscopy. *J. Magn. Reson.* 1985; **65**: 355–360.
18 Griesinger C, Otting G, Wüthrich K, Ernst RR. Clean TOCSY for proton spin system identification in macromolecules. *J. Am. Chem. Soc.* 1988; **110**: 7870–7872.
19 Bax A, Subramanian S. Sensitivity-enhanced two-dimensional heteronuclear shift correlation NMR spectroscopy. *J. Magn. Reson.* 1986; **67**: 565–569.
20 Bax A, Summers MF. Proton and carbon-13 assignments from sensitivity-enhanced detection of heteronuclear multiple-bond connectivity by 2D multiple quantum NMR. *J. Am. Chem. Soc.* 1986; **108**: 2093–2094.
21 Bauer C, Freeman R, Frenkiel T, Keeler J, Shak AJ. Gaussian pulses. *J. Magn. Reson.* 1984; **58**: 442–457.
22 Emsley L, Bodenhausen G. Self-refocusing effect of 27° Gaussian pulses. Applications to selective two-dimensional exchange spectroscopy. *J. Magn. Reson.* 1989; **82**: 211–221.
23 Bax A, Griffey RH, Hawkins BL. Correlation of proton and nitrogen-15 chemical shifts by multiple quantum NMR. *J. Magn. Reson.* 1983; **55**: 301–315.
24 Schwieters CD, Kuszewski JJ, Tjandra N, Clore GM. *J. Magn. Reson.* 2003; **160**: 65–74. (based on X-PLOR 3.851 by Brunger AT).
25 Korady R, Billeter M, Wüthrich K. *J. Mol. Graph.* 1996; **14**: 51–55.
26 El-Hajji M, Rebuffat S, Le Doan T, Klein G, Satre M, Bodo B. *Biochim. Biophys. Acta* 1989; **978**: 97–104.
27 Park Y, Park SN, Park SC, Park JY, Park YH, Hahm JS, Hahm K-S. *Biochem. Biophys. Res. Commun.* 2004; **321**: 631–637.

28 Carpino LA. 1-Hydroxy-7-azabenzotriazole. An efficient peptide coupling additive. *J. Am. Chem. Soc.* 1993; **115**: 4397–4398.
29 Podlech J. In *Houben-Weyl: Methods of Organic Chemistry, Synthesis of Peptides and Peptidomimetics*. Vol. E22a, Goodman M, Felix A, Moroder L, Toniolo C (eds). Thieme: Stuttgart, 2003; 517–533.
30 König W, Geiger R. Eine neue Methode zur Synthese von Peptiden: Aktivierung der Carboxylgruppe mit Dicyclohexylcarbodiimid unter Zusatz von 1-Hydroxy-benzotriazolen. *Chem. Ber.* 1970; **103**: 788–798.
31 Bellamy LJ. *The Infrared Spectra of Complex Molecules*. 2nd edn, Methuen: London, 1966.
32 Cung MT, Marraud M, Néel J. Étude expérimentale de la conformation de molécules dipeptidiques. Comparison avec les prévision théoriques. *Ann. Chim. (Paris)* 1972; 183–209.
33 Pysh E, Toniolo C. Conformational analysis of protected norvaline oligopeptides by high resolution proton magnetic resonance. *J. Am. Chem. Soc.* 1977; **99**: 6211–6219.
34 Karle IL, Balaram P. Structural characteristics of α-helical peptide molecules containing Aib residues. *Biochemistry* 1990; **29**: 6747–6756.
35 Di Blasio B, Pavone V, Saviano M, Lombardi A, Nastri F, Pedone C, Benedetti E, Crisma M, Anzolin M, Toniolo C. Structural characterization of the β-bend ribbon spiral: crystallographic analysis of two long (L-Pro-Aib)$_n$ sequential peptides. *J. Am. Chem. Soc.* 1992; **114**: 6273–6278.
36 Toniolo C, Crisma M, Formaggio F, Peggion C. Control of peptide conformation by the Thorpe – Ingold effect (C^{α}-tetrasubstitution). *Biopolymers (Pept. Sci.)* 2001; **60**: 396–419.
37 Beychok S. In *Poly-α-Amino Acids: Protein Models for Conformational Studies*. Fasman GD (ed). Dekker: New York, 1967; 293–337.
38 Manning MC, Woody RW. Theoretical CD studies of polypeptide helices: examination of important electronic and geometric factors. *Biopolymers* 1991; **31**: 569–585.
39 Toniolo C, Polese A, Formaggio F, Crisma M, Kamphuis J. Circular dichroism spectrum of a peptide 3_{10}-helix. *J. Am. Chem. Soc.* 1996; **118**: 2744–2745.
40 Formaggio F, Crisma M, Rossi P, Scrimin P, Kaptein B, Broxterman QB, Kamphuis J, Toniolo C. The first water-soluble 3_{10}-helical peptides. *Chem. Eur. J.* 2000; **6**: 4498–4504.
41 Teixeira V, Feio MJ, Rivas L, De la Torre BG, Andreu D, Coutinho A, Bastos M. Influence of lysine N^{ε}-trimethylation and lipid composition on the membrane activity of the cecropin A-melittin hybrid peptide CA(1–7)M(2–9). *J. Phys. Chem. B* 2010; **114**: 16198–16208.
42 Mills FD, Antharam VC, Ganesh OK, Elliott DW, Mc Neill SA, Long JR. The helical structure of surfactant peptide KL_4 when bound to POPC: POPG lipid vesicles. *Biochemistry* 2008; **47**: 8292–8300.
43 Chupin V, Leenhouts JM, de Kroon AIPM, de Kruiff B. Cardiolipin modulates the secondary structure of the presequence peptide of cytochrome oxidase subunit IV: a 2D ^{1}H-NMR study. *FEBS Lett.* 1995; **373**: 239–244.
44 Wallimann P, Kennedy RJ, Kemp DS. Large circular dichroism ellipticities for N-templated helical polypeptides are inconsistent with currently accepted helicity algorithms. *Angew. Chem. Int. Ed.* 1999; **38**: 1290–1292.
45 Chin D-H, Woody RW, Rohl CA, Baldwin RL. Circular dichroism spectra of short, fixed-nucleus alanine helices. *Proc. Natl. Acad. Sci. USA* 2002; **49**: 15416–15421.
46 Aravinda S, Datta S, Shamala N, Balaram P. Hydrogen-bond lengths in polypeptide helices: no evidence for short hydrogen bonds. *Angew. Chem. Int. Ed.* 2004; **43**: 6728–6731.
47 Wüthrich K. *NMR of Proteins and Nucleic Acids*. Wiley: New York, 1986.
48 Bellanda M, Peggion E, Bürgi R, van Gusteren WF, Mammi S. Conformational study of an Aib-rich peptide in DMSO by NMR. *J. Pept. Res.* 2001; **57**: 97–106.
49 Nguyen H-H, Imhof D, Kronen M, Schlegel B, Hrtl A, Gräfe U, Gera L, Reissmann S. Synthesis and biological evaluation of analogues of the peptaibol ampullosporin A. *J. Med. Chem.* 2002; **45**: 2781–2787.
50 Yamaguchi H, Kodama H, Osada S, Kato F, Jelokhani-Niaraki M, Kondo M. Effect of α,α-dialkyl amino acids on the protease resistance of peptides. *Biosci. Biotechnol. Biochem.* 2003; **67**: 2269–2272.
51 Sadowski JD, Murray JK, Tomita Y, Gellman SH. Exploration of backbone space in foldamers containing α- and β-amino acid residues: developing protease-resistant oligomers that bind tightly to the BH3-recognition cleft of Bcl-x_L. *ChemBioChem* 2007; **8**: 903–916.
52 De Zotti M, Biondi B, Formaggio F, Toniolo C, Stella L, Park Y, Hahm K-S. Trichogin GA IV: an antibacterial and protease-resistant peptide. *J. Pept. Sci.* 2009; **15**: 615–619.
53 Fox RO, Richards FM. A voltage-gated ion channel model inferred from the crystal structure of alamethicin at 1.5-Å resolution. *Nature* 1982; **300**: 325–330.
54 Crisma M, Peggion C, Baldini C, MacLean EJ, Vedovato N, Rispoli G, Toniolo C. Crystal structure of a spin-labeled, channel-forming alamethicin analogue. *Angew. Chem. Int. Ed.* 2007; **46**: 2047–2050 and references cited therein.
55 Bobone S, Bocchinfuso G, Palleschi A, Kim JY, Park Y, Hahm K-S, Stella L. In *Peptides 2010: Tales of Peptides*. Lebl M, Meldal M, Jensen KJ, Hoeg-Jensen T (eds). Prompt Scientific Publishing: San Diego, CA, 2010; 2010; 370–371.

